Analyst

Check for updates

Ultrasound combined with manganese-oxide nanoparticles loaded on activated carbon for extraction and pre-concentration of thymol and carvacrol in methanolic extracts of *Thymus daenensis*, *Salvia officinalis*, *Stachys pilifera*, *Satureja khuzistanica*, and mentha, and water samples†

Arash Asfaram, [ID] *[a] Hossein Sadeghi, [ID] [a] Alireza Goudarzi, [ID] [b] Esmaeel Panahi Kokhdan [ID] [a] and Zeinab Salehpour [ID] [a]

A dispersive micro solid-phase extraction (DMSPE) technique was developed using manganese-oxide nanoparticles loaded on activated carbon (Mn_3O_4-NPs-AC) as an effective sorbent combined with ultrasound for the extraction and determination of a trace amount of thymol and carvacrol in methanolic extracts of *Thymus daenensis*, *Salvia officinalis*, *Stachys pilifera*, *Satureja khuzistanica* and mentha, and water samples. Thymol and carvacrol phenolic compounds were extracted from real samples using acetonitrile (ACN) as the desorption solvent. Using central composite design (CCD), the effects of pH, ionic strength (NaCl), nano-sorbent mass, contact time, and desorption volume were investigated. Additionally, based on five-level variables, response surface methodology was used to determine the individual and interactive effects between factors on the process. The optimized extraction conditions included 12 mg of Mn_3O_4-NPs-AC as the sorbent, 300 μL of ACN as the desorption solvent, pH 3.0, 0.5 w/v% of NaCl, and 4.5 min sonication time. Under the optimized conditions, for all the samples, the limits of detection were $0.054-0.104$ ng mL^{-1} and the limits of quantification were $0.178-0.345$ ng mL^{-1}. The correlation coefficients of the calibration curves were >0.985, *i.e.* in the range of $0.4-6000$ ng mL^{-1}. To validate the effects of the matrix, the recovery, reproducibility, repeatability, and overall uncertainty were calculated for the five methanolic extracts, at 50, 100, and 500 ng mL^{-1}. The recovery ranged between 94.5% and 109.0% with a relative standard deviation of <8.0 for the repeatability and reproducibility precision, which strongly supports the favorable repeatability and reproducibility of the method. The presented method also has the excellent sorbent features of NPs for the sorption of the analyte, which is due to the use of ultrasound for dispersion of the material in the sample matrix.

1. Introduction

Antioxidants are natural compounds or substances having the ability to counteract chemically active products of metabolism.[1] In recent years, researchers have focused their attention on phenolic compounds because of their antioxidant activity in protecting the human body against free radicals.

Due to the presence of phenolic compounds, especially thymol and carvacrol, a large number of plants could help avoid a variety of diseases.[2,3]

Thymol and carvacrol are phenolic volatile monoterpenes found in essential oils of different herbs, chiefly at concentrations between 20% and 98%.[4,5] These two substances have been affirmed for their antimicrobial activity, mainly against Gram-positive microorganisms,[6] and have a wide range of applications in the food and veterinary industries, to combat antibiotic-resistant pathogenic microorganisms.[7]

Thymus daenensis,[8,9] *Salvia officinalis*,[10] *Stachys pilifera*,[11] *Satureja khuzistanica*,[12] and mentha are well-known plant species composed of thymol and carvacrol, together with their

[a]Medicinal Plants Research Center, Yasuj University of Medical Sciences, Yasuj, Iran. E-mail: arash.asfaram@yums.ac.ir

[b]Department of Polymer Engineering, Golestan University, Gorgan 49188-88369, Iran

†Electronic supplementary information (ESI) available. See DOI: 10.1039/c8an02338g

major components. Hence, developing a simple and an efficient method for the extraction and quantification of such antioxidants has been the goal of many scientists.[4,13,14]

High performance liquid chromatography (HPLC) has hitherto been the most popular method, owing to its relatively low cost and universality for the analysis of phenolic compounds.[13,15,16] However, prior to chromatographic analysis, due to the intricate matrix effect and the low levels of analytes in the actual samples, performing a simple and an efficient sample pretreatment process for the elimination of the interferents and enrichment of the analytes is highly required.[17–20]

Sample preparation is a key process before the analysis of organics in water samples.[21–23] In the selection of a sample preparation method, time consumption plays a central role since short time assists in enhancing the working efficiency.[24,25] Therefore, to attain ultrafast extraction, the diffusion distance both in the aqueous phase and in the extraction phase needs to be reduced in the shortest time, which means that the micro-extraction phase should be very small.[26] To achieve this goal, it is better for the micro-extraction phase to be well dispersed in the sample solution, rather than aggregated or stacked together. Hence, the diffusion distance in the sample solution could be diminished effectively at the micro level.[22,23,27,28]

More recently, a new method of solid-phase extraction (SPE), namely solid-phase microextraction (SPME), has been increasingly utilized.[29] Compared to traditional SPEs, SPME uses a trace of solid phase for extraction (*i.e.* of the order of μg), thereby minimizing the consumption of sorbent and maximizing the extraction process.[30] Dispersive micro-solid phase extraction (DMSPE) is one of the extraction techniques in which the volume of extraction phase is very small, and the extraction efficiency depends on the distribution of the target analytes between the extraction phase and the sample solution.[31] The greater the tendency of the analytes to accumulate in the extraction phase, the more is extracted, hence increasing the extraction efficiency. In the DMSPE method, in the extraction phase, the analyte is absorbed through a solid phase with the aid of magnetic stirring, vortexing, or ultrasonication. The analyte is then rinsed with a solvent or a mixture of organic solvents.[32] In this method, the mixture of the analytes by ultrasonication leads to an increase in mass transfer to the solid phase. In spite of the reduction in the volume of organic solvents in SPME, the use of ultrasound means that it is performed faster due to the formation of fine droplets and the increase in the contact surface between the two liquid transfer fluids. Therefore, new miniaturized approaches such as DMSPE provide numerous advantages such as suitability for analyzing very small amounts of analyte, consumption of small amounts of sorbent, and low use of toxic organic solvents.[33,34]

On the basis of our experiences with manganese-oxide nanoparticles (Mn_3O_4-NPs) and based on the data from the literature, these particles have the ability of strong surface complexing for sorption of phenolic compounds with fast kinetics. Physicochemically, they have also been shown to be highly

stable against acids, alkalis, oxidants, and reductants[35] and to be non-toxic and poorly soluble in water.[36] Application of metal nanomaterials has been demonstrated to elevate, to a great extent, the sorption capacities of phenolic compounds because of the special features of nano-scaled materials, *i.e.* high surface-area-to-volume ratio and homogeneous distribution in solution.[37,38] The presence of hydroxyl groups in phenolic molecules makes these molecules a good candidate for extraction from real matrices by Mn_3O_4-NPs.

In the DMSPE method, the extraction efficiency may be affected by various factors, especially type and volume of desorption solvent, pH, nano-sorbent mass, and extraction time. Therefore, it is important to optimize the extraction conditions.[39,40] To better examine the parameters in DMSPE using Mn_3O_4-NPs-AC, the procedures of experimental design are a preferable option.[41] By considering the interaction and quadratic effects, these procedures are able to fit second-order response surfaces, thereby optimizing the experimental conditions more effectively with relatively minimal experimental trials.[42,43]

A literature review indicates that no DMSPE method has been previously reported using Mn_3O_4-NPs loaded on activated carbon (Mn_3O_4-NPs-AC) for the extraction of phenolic compounds, including thymol and carvacrol. Therefore, in the present investigation, DMSPE was used to extract these phenolic compounds from *Thymus daenensis*, *Salvia officinalis*, *Stachys pilifera*, *Satureja khuzistanica*, mentha, and water samples prior to their determination by HPLC-UV. For this purpose, the effective parameters in the DMSPE extraction method for the two analytes were investigated and optimized by the experimental design approach, central composite design (CCD). The type of desorption solvent can be readily optimized by the one-variable-at-a-time approach. The DMSPE method was validated for precision, repeatability, recovery, and qualitative and quantitative limits and was employed to determine phenolic compounds.

2. Materials and methods

2.1. Reagents, solutions, and instrumental and operating conditions

Carvacrol (>98%) and thymol (≥98.5) were procured from Sigma-Aldrich (Saint Louis, MO; USA). The stock solutions of thymol and carvacrol (50 mg L^{-1}) were prepared by dissolving 5 mg of each phenolic compound in 100 mL of methanol (MeOH) and stored in a refrigerator at 4 °C. From these stock solutions, the standard working solutions were obtained daily by using double distilled water. Calibration curves (Fig. S1†) were constructed using different concentrations of the phenolic compounds in the range of 0.0005–2.0 mg L^{-1}. Manganese(II) acetate [$Mn(CH_3COO)_2$], ammonium acetate [$NH_4(CH_3COO)$], sodium sulfide (Na_2S), AC, and analytical or HPLC-grade organic solvents such as acetonitrile (ACN), MeOH, acetone (Ac), ethanol (EtOH), dimethyl sulfoxide (DMSO), dimethylformamide (DMF), tetrahydrofuran (THF),

and other reagents were purchased from Merck Company (Darmstadt, Germany).

HPLC was carried out using a Knauer system (Berlin, Zehlendarf, Germany), equipped with a UV-VIS 2500 Detector. The separation of analytes was performed on a Knauer column (4.6 mm diameter × 250 mm length, particle size of 5 μm, Eurospher 100-5 C18) with a pre-column (Eurospher 100-5 C_{18}). The mobile phase included 55% ACN and 45% (v/v) water, delivered from separate pumps. The flow rate remained at 1.1 mL min^{-1} with UV detection at 220 nm, and the column temperature was set at room temperature. All of the other instruments applied in this research have been fully described in our previous publications.[44,45]

2.2. Synthesis of DMSPE nano-sorbent

The preparation of Mn_3O_4-NPs-AC was carried out as follows: first 10.0 mL of 1.0 mol L^{-1} $Mn(CH_3COO)_2$ solution and 10.0 mL of 1 mol L^{-1} $NH_4(CH_3COO)$ solution were mixed with 5.0 mL of Na_2S solution and 5.0 mL of sodium hydroxide solution. To this mixture, deionized water was added to prepare 100 mL of total volume. The reaction solution was then preserved at 50 °C. After 24 h, the prepared NPs were first filtered, then rinsed several times with deionized water and finally dried at room temperature. In the next step, 0.15 g of the Mn_3O_4-NPs was dispersed in 250 mL of deionized water in an Erlenmeyer flask to form an insoluble suspension. Finally, the homogenous deposition of Mn_3O_4-NPs-AC was carried out by adding 10 g of AC to the prepared Mn_3O_4-NP suspension while stirring strongly at room temperature for 4 h. After filtering and rinsing several times with deionized water, the prepared Mn_3O_4-NPs-AC was rinsed, dried at the temperature of 50 °C and used as a sorbent for extraction experiments.

2.3. Preparation of real samples

All plant materials (*Thymus daenensis*, *Salvia officinalis*, *Stachys pilifera*, *Satureja khuzistanica*, and mentha) were gathered from Kohgiluyeh and Boyer-Ahmad Province, Yasuj, Iran, during the flowering season of the plant. After identification, the plant leaves were cleaned, shade dried and finely ground. The extract was prepared by successive maceration of the powder (100 g) with MeOH/water (80 : 20%; to give 10 g of the extract) at room temperature (25 ± 2 °C) for 48 h. Following filtration, the evaporation of the extract was done in a rotary evaporator under low pressure (45 °C).[45] The extract was stored at −4 °C from where it was used when required. The dried extract material (0.01 g) was dissolved in MeOH (50 mL) in an ultrasonic bath device for 10 min for daily use in our extraction experiments. The dissolved extract, which was centrifuged at 6000 rpm for 15 min, was filtered through filter paper as well as through a 0.45 μm membrane filter (Millipore, USA).

2.4. Analytical procedure

DMSPE experiments were conducted in a 15 mL centrifuge tube. First, 12 mg of Mn_3O_4-NPs-AC was dispersed into 15 mL of standard solution containing 100 ng mL^{-1} of each phenolic compound, and the pH of the mixture was set to 3.0 with HCl/

NaOH. For the complete adsorption of the analytes, the tube was immersed in an ultrasound bath for 4.5 min. Subsequently, the isolation of sorbent from the solution was performed by centrifugation at 4000 rpm for 5 min. After discarding the supernatant, the adsorbed thymol and carvacrol were eluted from the sorbent with 300 μL ACN under vortexing for 2 min. After centrifugation at 4000 rpm for 5 min, the eluted phase was collected and filtered by the use of a Whatman 0.22 μm syringe filter. Finally, 20 μL of the eluted phase was injected into HPLC for analysis. Each experiment was repeated at least three times, and the results are reported as the mean value of these three experiments.

In this study, various extraction-controlling parameters (pH, nano-sorbent mass, extraction time, ionic strength (NaCl), and desorption volume) were optimized by response surface methodology (RSM)-based CCD. For each variable, five levels (0, −α, +α, −1, and +1) were assigned as the central points, low axial runs, high axial runs, low fractional factorials, and high fractional factorials, respectively, based on the CCD principle. The percentages of extraction recovery (ER%) of carvacrol and thymol were chosen as the response variables, whereas solid pH (X_1), ionic strength (X_2), nano-sorbent mass (X_3), extraction time (X_4), and desorption volume (X_5) were selected as the independent variables. The obtained experimental data fitted to the second-order polynomial model have been fully explained in our and other previous investigations.[46,47]

In this well-designed CCD model, with the goal of maximizing the recovery of thymol and carvacrol, we analyzed the impacts of the five independent variables on the response functions and evaluated the optimal preparation conditions. To ensure the accuracy of the model, conducting analysis of variance (ANOVA) is necessary; therefore, we used this method to affirm the linear, quadratic and interaction regression coefficients, individually. The statistical analysis of the computed *F*-value at $P < 0.05$ was performed in order to evaluate the importance of the dependent variables. Two variables that showed interactive effects on the process responses were maintained at the same time by fixing the other variable at its central point (*i.e.* 0). These effects were depicted using the 3D response surface plots drawn based on the fitted quadratic equation.

3. Results and discussion

3.1. Characteristics of the nano-sorbent

SEM images of the prepared Mn_3O_4-NPs-AC at different magnifications (Fig. 1) reveal that the Mn_3O_4-NPs-AC is formed from spherical shaped NPs with diameters of about 40–80 nm.

Fig. 2a shows the histogram of Mn_3O_4-NP size distribution. The diameters of the Mn_3O_4-NPs were in a wide range of 30–70 nm. The average diameter of the Mn_3O_4-NPs was 58 nm, which was close to the SEM result. The chemical composition of the prepared Mn_3O_4-NPs-AC was studied by energy dispersive X-ray (EDX) analysis. The C, Mn, and O peaks detected in

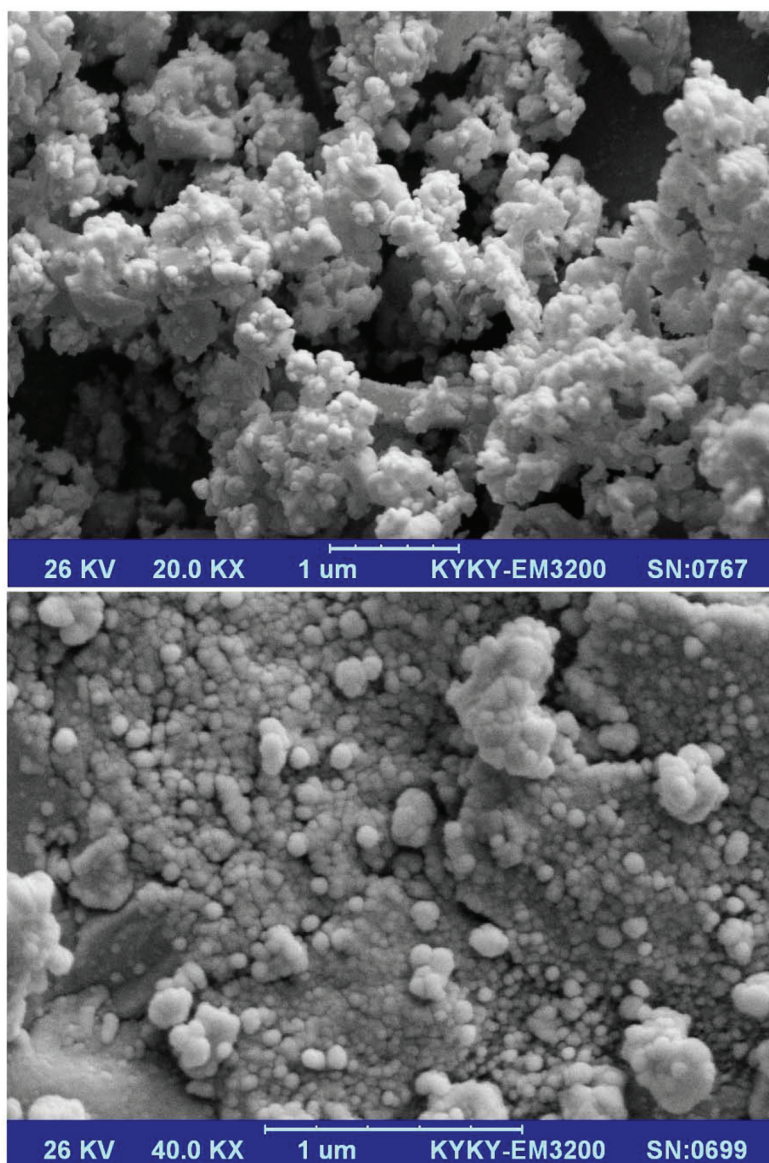**Fig. 1** SEM images of Mn_3O_4-NPs-AC at different magnifications.

the EDX spectrum of the Mn_3O_4-NPs-AC are shown in Fig. 2b. These results confirmed that the particles were composed of manganese and oxygen elements.

The type IV isotherm patterns with H3 hysteresis loops can be observed from the adsorption/desorption curves of the nano-sorbent, which shows a mesoporous structure (Fig. 2c). The Brunauer–Emmett–Teller surface area of the nano-sorbent is 310 m^2 g^{-1}, and the total pore volume is 0.392 cm^3 g^{-1}.

The X-ray diffraction (XRD) pattern of the prepared Mn_3O_4-NPs-AC was investigated in the 2θ region of 10–80°. According to the XRD pattern (Fig. 2d), the diffraction peak at 2θ of 24.0° was attributed to the planar structure of AC. Likewise, all of the characteristic diffraction peaks of a pure tetragonal crystal of Mn_3O_4-NPs at 2θ of 18.0° (101), 28.88° (112), 31.016° (200), 32.32° (103), 36.10° (211), 36.45° (202), 38.00° (004), 44.45° (220), 49.82° (204), 50.71° (105), 53.86° (312), 56.01° (303),

58.51° (321), 59.84° (224), 64.65° (400), 69.66° (305), 74.15° (413), 76.58° (422), and 77.51° (404) were also present for the Mn_3O_4-NPs-AC, further indicating the successful synthesis of Mn_3O_4-NPs-AC, based on the good agreement with JCPDS card (No. 24-0734).

3.2. Selection of the desorption solvent

The elution is a key step for obtaining good recovery and recyclability of the sorbent material; however, incomplete elution results in a carry-over effect and restricts the use of the material. Elution solvent polarity is a crucial factor in the process of solvent selection. According to the principle of "like dissolves like", a good agreement between the polarities of the desorption solvents and the target analytes is required to lead to better desorption efficiency. Various elution solvents, *viz.* ACN, Ac, MeOH, THF, EtOH, DMF, and DMSO, were used to
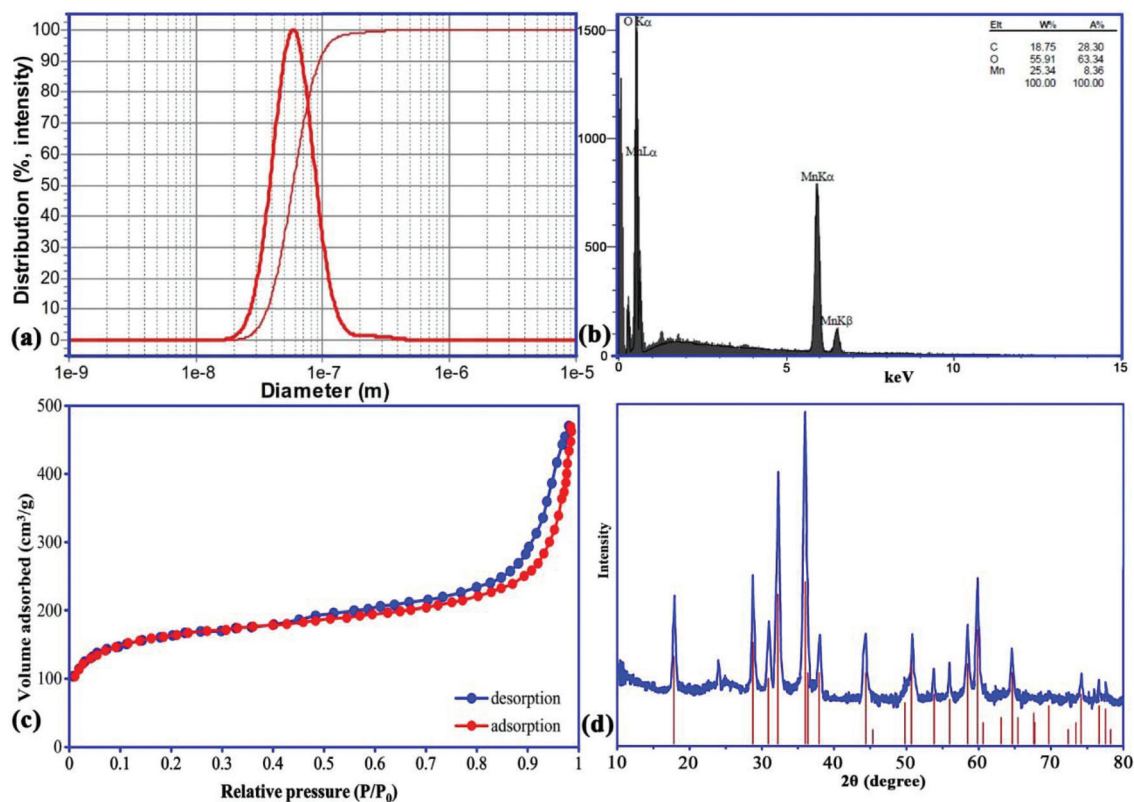
Fig. 2 Particle size distribution (a), EDX analysis (b), N_2 adsorption/desorption isotherms (c), and XRD pattern (d) of Mn_3O_4-NPs-AC.

desorb the phenolic compounds from the nano-sorbent; the highest extraction efficiency of each analyte was obtained when ACN was selected as the desorption solvent (Fig. 3). To investigate the effect of volume of solvent on desorption, further experiments were done by eluting the analytes with different amounts of ACN (50–350 μL).

3.3. Statistical design of experiments

3.3.1. CCD and fitted regression. The total number of runs ($n = 32$) in CCD and the output responses for the carvacrol and thymol, as analyte extraction, are shown in Table S1.†

To attain an estimation of the pure error variance, we used three replicate runs at the center of the design. Using multiple
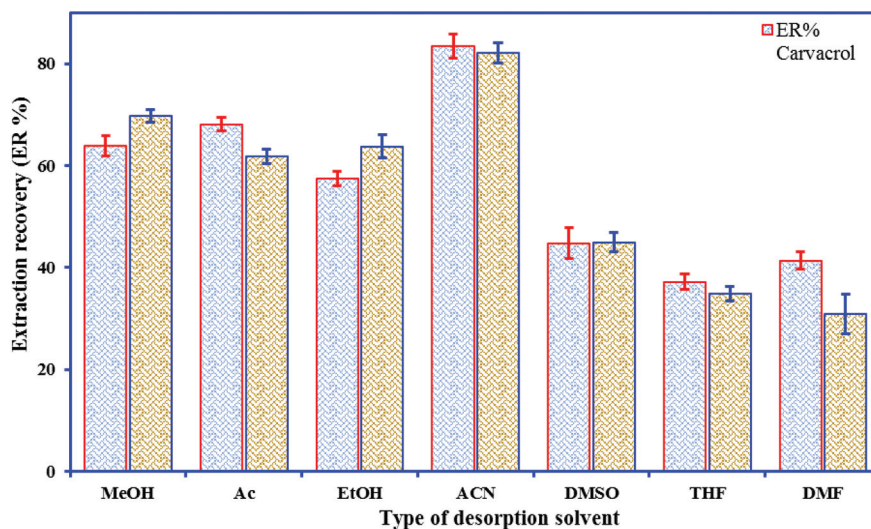

Fig. 3 Selection of the desorption solvent for the DMSPE experiments. Conditions: sample volume, 15.0 mL; desorption volume, 200 μL; extraction time, 3 min; nano-sorbent mass, 10 mg; desorption time, 3 min; pH, 5.0; room temperature.

regression analysis, the responses (carvacrol and thymol extraction) were closely related to all five design factors by using the second-order polynomial. Meanwhile, the quadratic regression models for ER% carvacrol and ER% thymol in terms of actual factors such as pH (X_1), ionic strength (X_2), nano-sorbent mass (X_3), extraction time (X_4), and desorption volume (X_5) are given by eqn (1) and (2), respectively:

$$\text{ER\%}_{\text{Carvacrol}} = 110.4 + 1.9X_1 - 5.9X_3 - 3.3X_4 + 0.02X_5 + 0.91X_1X_4 \\ - 0.03X_1X_5 + 5.0X_2X_3 - 5.4X_2X_4 + 0.2X_2X_5 + 0.6X_3X_4 \\ + 0.02X_3X_5 + 0.04X_4X_5 - 1.4X_1{}^2 - 1.067X_4{}^2$$

$$(1)$$

$$\text{ER\%}_{\text{Thymol}} = 119 + 0.4X_1 - 0.1X_3 - 9.8X_4 + 0.1X_5 + 7.3X_1X_2 \\ + 0.7X_1X_4 - 0.03X_1X_5 + 12.4X_2X_3 + 4.7X_2X_4 \\ + 0.6X_3X_4 + 0.02X_3X_5 + 0.03X_4X_5 - 1.2X_1{}^2 \\ - 68.0X_2{}^2 - 0.6X_3{}^2 - 0.6X_4{}^2$$

$$(2)$$

The significance and the fitness of the models was tested by ANOVA (Table S2†). The high "Model F-values" (59.69 for carvacrol and 43.66 for thymol) suggest that the models are significant, and there is a 0.01% chance of "Model F-values" this large happening owing to noise.[45]

The "Lack of Fit F-values" of 2.72 and 4.82 for carvacrol and thymol, respectively, reveal that the models are insignificant; there is a chance of 14.6% for carvacrol and 5.3% for thymol that the "Lack of Fit F-value" occurred because of noise.[18] The high values of correlation coefficient (R^2; 0.991 for carvacrol and 0.990 for thymol) for eqn (1) and (2) show the significance of the models and indicate a good connection between the observed values and the predicted values of the responses (Fig. 4).

In this study, X_2, $X_2{}^2$, X_1X_2, X_2X_3, and $X_3{}^2$ for carvacrol and X_2, X_2X_5, and X_1X_3 for thymol were not significant factors for both responses. On the contrary, X_1, X_3, and X_4 were signifi-

cant for both responses. The resulting effects and the significance of each factor are observable using a Pareto chart (Fig. S2†). Using this chart, it is feasible to accentuate the significant factors exceeding the vertical line ($P = 0.05$). Moreover, it is possible to detect the relationship and the magnitude of the effect of these factors, which is described by the signal and the value on each horizontal bar.

The adequate precision, a signal/noise ratio measuring the errors in the predictions at the design points, was found to be in the desirable range (<4).[29] The values of adequate precision were obtained as 30.68 and 26.70 for carvacrol and thymol, respectively, suggesting the capability of the developed quadratic models in navigation of the CCD design. The value of the coefficient of variance, which represents the error between the observed data and predicted data, was observed to be 4.6% for both responses. In addition, the value of coefficient of variance was <10%, which showed that the error in the model is non-significant.[48]

3.3.2. RSM plots of the carvacrol and thymol recovery. The association between the dependent variables and independent variables was clarified by constructing response surface plots (Fig. 5). In the regression model, there are five independent variables; one variable was kept fixed at the center level for each plot; therefore, a total of four response surface plots were produced for the responses.

As it is apparent from Fig. 5, the responses of both thymol and carvacrol reduce with pH elevation for all of the target solutions. The reason for this phenomenon could be due to the presence of carboxyl and hydroxyl groups on the sorbent, which can be ionized at high pH. These two groups are polar acidic, and at low pH, they are in the neutral form; therefore, both carboxyl and hydroxyl groups are appropriate for adsorption of polar analytes such as thymol and carvacrol. The highest extraction efficiency for the proposed nano-sorbent was achieved at pH 3.0 (Fig. 5a and b). Basically, in aqueous
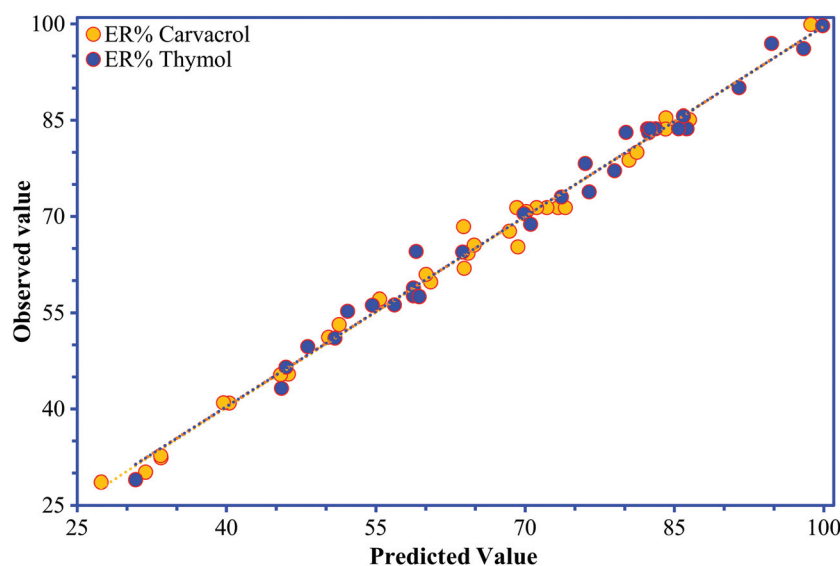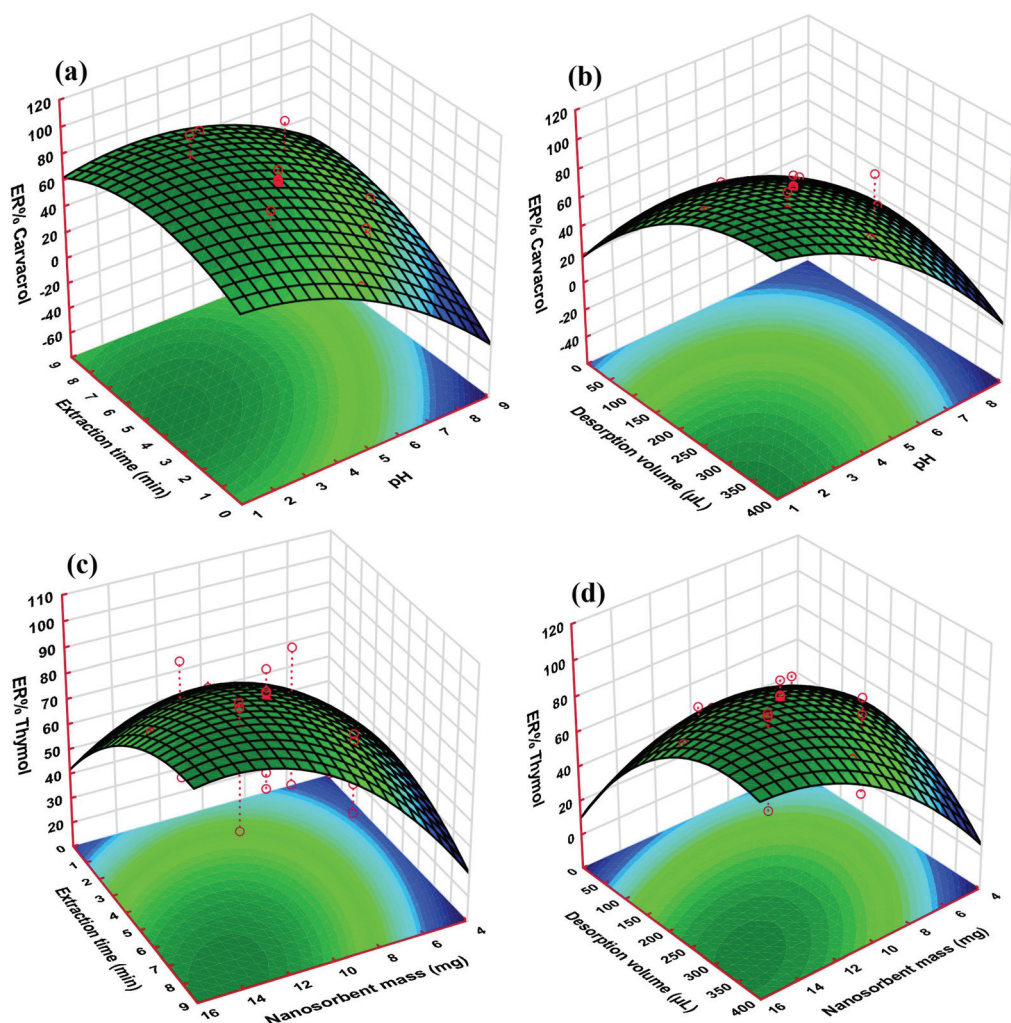

Fig. 4 The observed values for thymol and carvacrol determination plotted against the predicted values calculated from the CCD.

Fig. 5 Response surface plots of the interaction effect of different parameters on thymol and carvacrol recovery. (a) Interactive effect of pH and extraction time, (b) interactive effect of pH and desorption volume, (c) interactive effect of extraction time and nano-sorbent mass, and (d) interactive effect of desorption volume and nano-sorbent mass.

solutions, the speciation of compounds that are weakly acidic is related to the solution properties, *i.e.* its pH value. It has been demonstrated that acidification of water solutions can reduce the dissociation of weakly acidic analytes, which may raise the extraction efficiency of the target compounds in the case of the strong binding of the non-dissociated form to the sorbent.[49,50] In this situation, these acidic drugs have an interaction with the nano-sorbent surface through hydrophobic and π interactions, as well as hydrogen-bond formation.[51]

The enhancement of the extraction efficiency depends on time up to 4.5 min (Fig. 5a and c). This result demonstrated that 4.5 min is sufficient time for the complete equilibration of the sample solution and the sorbent. Therefore, this time was chosen as the optimal extraction time for further studies, since it is supposed to be able to achieve a balance between the extraction amount and the extraction time. However, extraction times longer than 4.5 min decrease the extraction

efficiency, which is likely due to interchange of adsorbed analytes and other species in the aqueous solution.

As can be seen in Fig. 5c and d, the ER of the analytes increased with nano-sorbent mass, which is because of the high specific surface area and small particle size of the sorbent. The extraction rate increased noticeably at a greater surface area and ratio of analyte to available sorption sites. On the other hand, nano-sorbents such as Mn_3O_4-NPs-AC have a high surface-area-to-volume ratio; therefore, the diffusion route of the analytes is short, which results in rapid and high extraction performance.

The desorption solvent volume in DMSPE has two opposite effects on the extraction efficiency. This means that with the elevation of the solvent volume, the solid–liquid equilibrium of the analytes shifts to the solvent phase, and, therefore, dilution of the final extract increases. In other words, the elevation of the solvent volume causes an increase in the extraction efficiency (Fig. 5b and d).

3.3.3. Optimization of the process parameters. According to the quadratic model, the estimated optimum conditions for the extraction of carvacrol and thymol from real samples are as follows: pH, 3.0; nano-sorbent mass, 12 mg; desorption volume; 300 μL; extraction time, 4.5 min, and NaCl, 0.5 w/v% (Fig. S3†).

Experiments were performed in triplicate under the optimal extraction conditions, and a comparison was carried out between the mean values of the observed results and the predicted values. Under the optimum conditions, the extraction amounts of carvacrol and thymol from real samples were 98.89% and 99.45%, respectively, which were close to the predicted value of 100%. The results obtained from confirmation experiments indicated that the model is adequate for predicting the expected optimization.

3.4. Method evaluation and real sample analysis

3.4.1. Evaluation of method performance. Under the optimized conditions, the performance of the developed Mn_3O_4-NPs-AC-based DMSPE method was evaluated to determine the two phenols in real samples. The results are presented in Table S3,† including limits of detection (LODs), limits of quantification (LOQs), linear ranges, R^2, enrichment factor (EFs), repeatability, and reproducibility of the developed method. As illustrated in Table S3,† the method showed good linearity, in the range from 0.4 to 6000 ng mL^{-1}, and the R^2 of

the linearity was in the range of 0.985–0.999. The LODs and LOQs of the proposed method, calculated based on the signal-to-noise ratio of 3 and 10, respectively, were in the range of 0.054–0.104 ng mL^{-1} and 0.178–0.345 ng mL^{-1}, respectively. The EFs of the two phenols ranged from 100.5 to 222.80.

3.4.2. Application to medical plants and water samples. The applicability of the method to real samples was evaluated by our developed Mn_3O_4-NPs-AC-based DMSPE method in order to detect the two phenolic compounds in extracts of plants. The recovery of the proposed method was validated by DMSPE of the two phenols spiked at three concentration levels (50, 100, and 500 ng mL^{-1}), and the results are shown in Tables 1 and 2.

The obtained extraction recoveries were used to evaluate the accuracy of the model, which ranged from 94.49 to 108.97% with the relative standard deviation (RSD) in the range of 1.37–7.80%. As displayed in Tables 1 and 2, the repeatability for carvacrol and thymol standard solutions was evaluated with three different injections of spiked real samples at three concentration levels (50, 100, and 500 ng mL^{-1}), and the obtained RSD values of ER% were in the range of 1.37–5.20%. The reproducibility was evaluated in the same laboratory but conducted by different operators and under different environmental conditions on three separate days, and the obtained RSD ranged from 1.62% to 7.80%. These results further con-

Table 1 Results of carvacrol and thymol determination in real samples[a]

Real samples	Added (ng mL^{-1})	Found (ng mL^{-1})		RR%[b]		RSD (%)	
		Carvacrol	Thymol	Carvacrol	Thymol	Carvacrol	Thymol
Double-distilled water	0.0	ND[c]	ND	—	—	—	—
	50	49.78	49.92	99.55	99.85	2.52	2.56
	100	102.58	101.64	102.58	101.64	3.19	3.34
	500	495.19	493.16	99.04	98.63	1.39	1.37
Thymus daenensis Celak	0.0	81.70	101.69	—	—	—	—
	50	135.82	153.28	108.24	103.17	4.41	4.80
	100	184.55	198.04	102.85	96.35	4.75	3.58
	500	577.37	615.41	99.13	102.74	1.91	5.20
Salvia officinalis	0.0	33.29	31.59	—	—	—	—
	50	85.64	83.07	104.70	102.97	4.23	5.12
	100	128.01	137.57	94.72	105.98	3.60	2.42
	500	541.85	524.36	101.71	98.55	1.41	1.54
Stachys pilifera	0.0	109.91	55.47	—	—	—	—
	50	159.26	102.71	98.70	94.49	3.55	3.96
	100	212.62	158.19	102.71	102.72	2.71	4.54
	500	632.53	554.78	104.52	99.86	1.97	2.18
Satureja khuzistanica	0.0	76.32	76.47	—	—	—	—
	50	127.98	127.42	103.33	101.89	4.49	3.50
	100	171.54	178.83	95.22	102.36	2.89	5.00
	500	575.02	591.27	99.74	102.96	2.33	4.04
Mentha	0.0	68.78	6.08	—	—	—	—
	50	117.37	57.27	97.18	102.37	2.22	2.44
	100	173.04	110.48	104.26	104.40	4.14	4.44
	500	566.44	519.68	99.53	102.72	1.56	3.06

[a] Intra-day. [b] Relative recovery (RR%). [c] Not detected.

Table 2 Results of carvacrol and thymol determination in real samples[a]

Real samples	Added (ng mL⁻¹)	Found (ng mL⁻¹)		RR%[b]		RSD (%)	
		Carvacrol	Thymol	Carvacrol	Thymol	Carvacrol	Thymol
Double-distilled water	0.0	ND[c]	ND	—	—	—	—
	50	51.11	50.19	102.22	100.38	2.37	5.03
	100	98.43	99.90	98.43	99.90	1.62	3.03
	500	500.97	511.45	100.19	102.29	2.18	4.81
Thymus daenensis Celak	0.0	81.70	101.69	—	—	—	—
	50	131.76	155.14	100.11	106.90	7.80	6.98
	100	177.41	203.67	95.71	101.98	2.47	6.55
	500	593.55	583.20	102.37	96.30	4.63	5.67
Salvia officinalis	0.0	33.29	31.59	—	—	—	—
	50	87.25	83.41	107.93	103.65	6.69	5.04
	100	128.41	128.08	95.12	96.49	5.01	3.34
	500	548.77	537.75	103.10	101.23	3.73	7.56
Stachys pilifera	0.0	109.91	55.47	—	—	—	—
	50	157.49	103.68	95.15	96.41	6.02	7.15
	100	211.65	157.44	101.74	101.97	2.29	3.18
	500	601.58	568.81	98.33	102.67	5.50	6.98
Satureja khuzistanica	0.0	76.32	76.47	—	—	—	—
	50	130.27	129.49	107.91	106.03	5.08	4.91
	100	179.42	171.38	103.10	94.91	4.39	5.33
	500	557.12	600.94	96.16	104.89	2.21	4.11
Mentha	0.0	68.78	6.08	—	—	—	—
	50	123.26	58.80	108.97	105.44	4.31	5.76
	100	163.55	103.64	94.77	97.56	6.65	6.35
	500	600.00	481.82	106.24	95.15	7.27	7.22

[a] Inter-day. [b] Relative recovery (RR%). [c] Not detected.

Table 3 Comparison of the method presented in this study with other reported methods for the determination of the selected phenolic compounds

Method	Sample preparation	Sample	ER (%)	Precision (% RSD)	LOD (ng mL⁻¹)	LOQ (ng mL⁻¹)	Linear range (ng mL⁻¹)	Time (min)	Ref.
HPLC-UV	SPE	*Thymus vulgaris* L. volatile oil	96.70–98.70	0.80–0.490	0.6–1.8	2.8–8.6	2.0–90 000	>30	14
GC-FID	SPE								
GC-FID	HS-SPME	Human plasma	81.0–118.0	3.87–18.0	8.1	15	8.1–203.5	35	52
GC-FID	HD-HSME	*Thymus transcaspicus*	89.0–116.0	2.3–9.56	230–1870	77–6230	1250–87 500	50	9
HPLC-UV	UAME-NMSPD	Broncho T.D. syrup Thymian syrup	94.50–99.40	2.66–4.93	0.21–0.23	—	5.0–2000	15	15
HPLC-UV	VASEDLLME	Broncho T.D. syrup Thymian syrup Distilled thyme	93.8–105.2	1.02–4.85	0.160	0.500	5.0–4000	10	20
HPLC-UV	Electrochemical	Peppermint oil Basil oil Oregano oil Clove oil	99.0–108.0	3.00–15.0	0.81–5.0	2.70–57.0	10–10 000	30	53
HPLC-UV	SPME	Thyme, Savory, Honey	94.00–119.0	6.80–12.70	0.60–0.80	—	1.0–80	>120	13
GC-MS	HS-SPME	Plasma; milk	—	2.00–16.00	0.31–0.89	—	2.0–400.0	40	4
HPLC-UV	DMSPE	–*Thymus daenensis* –*Salvia officinalis* –*Stachys pilifera* –*Satureja khuzistanica* –Mentha –Water samples	94.49–108.97	1.37–7.80	0.054–0.104	0.178–0.345	0.4–6000	<10	This work

HPLC-UV: High-performance liquid chromatography UV detector. SPE: Solid-phase extraction. GC-FID: Gas chromatography coupled with flame ionization detector. HS-SPME: Headspace solid phase microextraction. HD-HSME: Hydro distillation-headspace solvent microextraction. UAME-NMSPD: Ultrasound-assisted microextraction-nanomaterial solid-phase dispersion. VASEDLLME: Vortex-assisted surfactant-enhanced dispersive liquid–liquid microextraction. GC-MS: Gas chromatography-mass spectrometry. SPME: Solid-phase microextraction. DMSPE: Dispersive micro-solid phase extraction.

firmed the good repeatability and reproducibility of the proposed method.

3.4.3. Comparison with other methods. Comparison of the proposed method with other techniques in terms of LODs, LOQs, recoveries, linear range, RSDs, and extraction time (Table 3) revealed that our developed method has a wide linear range, low LOD, and good reproducibility compared to other reported methods. The Mn_3O_4-NPs-AC-based DMSPE method also has some other significant merits, such as saving of time, providing an efficient procedure for lowering the costs, and being involved in the control of two phenols in real samples. The presented method is also more environmentally friendly and uses less toxic reagents in comparison to the methods in

the literature that need a lot of organic solvents. Hence, it is apparent that the presented HPLC-UV technique with the Mn_3O_4-NPs-AC-based DMSPE preparation process is a simple, rapid, eco-friendly, and robust method suitable for the analysis of carvacrol and thymol in different real samples.

Fig. 6 and Fig. S4–S8† show the chromatograms obtained using the Mn_3O_4-NPs-AC-based DMSPE method coupled with HPLC-UV for two target compounds in real samples at the spiking concentration of 100 ng mL^{-1}.

3.5. Reusability of the nano-sorbent

The reusability of the nano-sorbent material is key and an effective indicator used in the extraction processes. This cri-
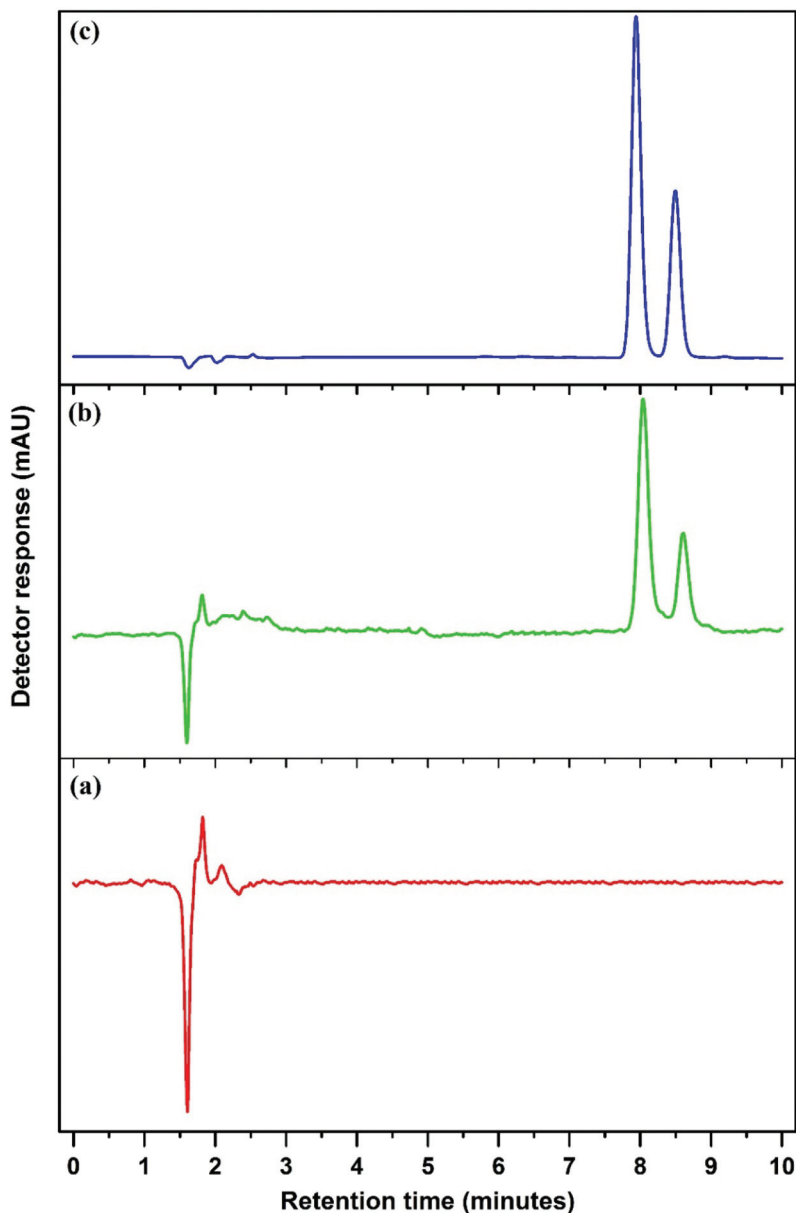
Fig. 6 Typical chromatogram obtained for the extraction of a water sample spiked with the two analytes under the optimum conditions: (a) non-spiked, (b) spiked with 100 ng mL^{-1} before DMSPE, and (c) extracted from a water sample after DMSPE of the analytes.

terion suggests the regeneration efficiency and also the cost-effectiveness of the system. To evaluate the extraction re-usability of Mn_3O_4-NPs-AC, the material was reused for several extraction experiments. Fig. S9† shows the recycling efficiency of the Mn_3O_4-NPs-AC. Under the same experimental conditions, the sorbent can be used for the recovery of two compounds. After the sixth cycle, only 8.0% and 3.0% of the carvacrol and thymol compounds were liberated from the sorbent, respectively, depicting that the prepared nano-sorbent can be used as a high-performance recyclable sorbent for DMSPE applications.

4. Conclusions

Using Mn_3O_4-NPs-AC in combination with HPLC-UV, a method was developed for the DMSPE and determination of carvacrol and thymol in medical extracts of plants and water samples. This new methodology provided excellent recoveries for the two phenolic compounds, showing the applicability of the method for medical extract analysis. The presented technique also provides efficient enrichment of the extract and allows the required sensitivity using HPLC and UV-Vis as a detector. In the current work, a five-level-five-factor CCD combined with RSM experiments was used for the optimization of the ER of the two phenolic compounds. Under the optimal conditions, the developed method demonstrated low LODs (0.054–0.104 ng mL^{-1}), good precision (<8.0%), good repeatability (1.37–5.20%), a wide linear range (0.4–6000 ng mL^{-1}, R^2 > 985%), and good EFs (100.5–222.80) for detecting the two phenols. Additionally, the method was successfully applied in the detection of the two phenols in medical extracts of plants and water samples with satisfactory recoveries (94.49–108.97%). Owing to the π–π stacking interactions and H-bonding between the oxygen-rich functional groups of the activated carbon and the hydroxyl groups of the phenol analytes, the Mn_3O_4-NPs-AC nano-sorbent exhibited great extraction performance for the two phenols. Taken together, the novelty of the present investigation is the use of a nano-material, namely Mn_3O_4-NPs-AC, as a sorbent for the analysis of phenol compounds. The nano-properties of the sorbent allow a small nano-sorbent mass to be used without loss of efficiency and enable its application in real samples. Based on our results, this technique is suitable for the determination of a trace amount of thymol and carvacrol in methanolic extracts of plants and water samples.

Conflicts of interest

All authors declare no conflicts of interest.

Acknowledgements

References

1 C. Lopez-Alarcon and A. Denicola, *Anal. Chim. Acta*, 2013, **763**, 1–10.
2 M. Bergman, L. Varshavsky, H. E. Gottlieb and S. Grossman, *Phytochemistry*, 2001, **58**, 143–152.
3 L. Rubio, M.-J. Motilva and M.-P. Romero, *Crit. Rev. Food Sci. Nutr.*, 2013, **53**, 943–953.
4 G. M. L. Fiori, P. S. Bonato, M. P. M. Pereira, S. H. T. Contini and A. M. S. Pereira, *J. Braz. Chem. Soc.*, 2013, **24**, 837–846.
5 K. Can Baser, *Curr. Pharm. Des.*, 2008, **14**, 3106–3119.
6 M. Botelho, N. Nogueira, G. Bastos, S. Fonseca, T. Lemos, F. Matos, D. Montenegro, J. Heukelbach, V. Rao and G. Brito, *Braz. J. Med. Biol. Res.*, 2007, **40**, 349–356.
7 S. A. Baskaran, G. Kazmer, L. Hinckley, S. Andrew and K. Venkitanarayanan, *J. Dairy Sci.*, 2009, **92**, 1423–1429.
8 A. Pirbalouti, M. Rahimmalek, F. Malekpoor and A. Karimi, *Plant Omics*, 2011, **4**, 209.
9 V. Kiyanpour, A. R. Fakhari, R. Alizadeh, B. Asghari and M. Jalali-Heravi, *Talanta*, 2009, **79**, 695–699.
10 L. Pizzale, R. Bortolomeazzi, S. Vichi, E. Überegger and L. S. Conte, *J. Sci. Food Agric.*, 2002, **82**, 1645–1651.
11 K. Javidnia, R. Miri, M. Moein, M. Kamalinejad and H. Sarkarzadeh, *J. Essent. Oil Res.*, 2006, **18**, 275–277.
12 H. Farsam, M. Amanlou, M. Radpour, A. Salehinia and A. Shafiee, *Flavour Fragrance J.*, 2004, **19**, 308–310.
13 A. Ghiasvand, S. Dowlatshah, N. Nouraei, N. Heidari and F. Yazdankhah, *J. Chromatogr. A*, 2015, **1406**, 87–93.
14 H. Hajimehdipoor, M. Shekarchi, M. Khanavi, N. Adib and M. Amri, *Pharmacogn. Mag.*, 2010, **6**, 154–158.
15 M. Roosta, M. Ghaedi, A. Daneshfar and R. Sahraei, *J. Chromatogr. B: Anal. Technol. Biomed. Life Sci.*, 2015, **975**, 34–39.
16 L. I. Alekseeva, *Pharm. Chem. J.*, 2009, **43**, 665–667.
17 Y. Tong, X. Liu and L. Zhang, *Food Chem.*, 2019, **277**, 579–585.
18 A. Asfaram, M. Ghaedi, H. Abidi, H. Javadian, M. Zoladl and F. Sadeghfar, *Ultrason. Sonochem.*, 2018, **44**, 240–250.
19 N. Jalilian, H. Ebrahimzadeh and A. A. Asgharinezhad, *J. Chromatogr. A*, 2017, **1499**, 38–47.
20 M. Ghaedi, M. Roosta, S. Khodadoust and A. Daneshfar, *J. Chromatogr. Sci.*, 2015, **53**, 1222–1231.
21 K. Madej, T. K. Kalenik and W. Piekoszewski, *Food Chem.*, 2018, **269**, 527–541.
22 M. R. Gama and C. B. Bottoli, *J. Chromatogr. B: Anal. Technol. Biomed. Life Sci.*, 2017, **1043**, 107–121.
23 M. Ahmadi, H. Elmongy, T. Madrakian and M. Abdel-Rehim, *Anal. Chim. Acta*, 2017, **958**, 1–21.
24 M. Tuzen and M. Soylak, *J. Hazard. Mater.*, 2009, **164**, 1428–1432.
25 L. Xu, X. Qi, X. Li, Y. Bai and H. Liu, *Talanta*, 2016, **146**, 714–726.
26 J. Chen, Y. Wang, Y. Huang, K. Xu, N. Li, Q. Wen and Y. Zhou, *Analyst*, 2015, **140**, 3474–3483.

27 L.-J. Du, C. Chu, E. Warner, Q.-Y. Wang, Y.-H. Hu, K.-J. Chai, J. Cao, L.-Q. Peng, Y.-B. Chen, J. Yang and Q.-D. Zhang, *J. Chromatogr. A*, 2018, **1561**, 1–12.

28 L. Novakova and H. Vlckova, *Anal. Chim. Acta*, 2009, **656**, 8–35.

29 A. Salemi, N. Khaleghifar and N. Mirikaram, *Microchem. J.*, 2019, **144**, 215–220.

30 M. Ghani, S. Masoum, S. M. Ghoreishi, V. Cerdà and F. Maya, *J. Chromatogr. A*, 2018, **1567**, 55–63.

31 A. Asfaram, M. Ghaedi, A. Goudarzi, M. Soylak and S. Langroodi, *New J. Chem.*, 2015, **39**, 9813–9823.

32 T. Wang, J. Wang, C. Zhang, Z. Yang, X. Dai, M. Cheng and X. Hou, *Analyst*, 2015, **140**, 5308–5316.

33 C. Lou, C. Wu, K. Zhang, D. Guo, L. Jiang, Y. Lu and Y. Zhu, *J. Chromatogr. A*, 2018, **1550**, 45–56.

34 Z. Shi, D. Xu, X. Zhao, X. Li, H. Shen, B. Yang and H. Zhang, *J. Sep. Sci.*, 2017, **40**, 4591–4598.

35 E. Saputra, S. Muhammad, H. Sun, H.-M. Ang, M. O. Tadé and S. Wang, *J. Colloid Interface Sci.*, 2013, **407**, 467–473.

36 J. W. Lee, A. S. Hall, J.-D. Kim and T. E. Mallouk, *Chem. Mater.*, 2012, **24**, 1158–1164.

37 S.-Y. Liu, J. Xie, Y.-X. Zheng, G.-S. Cao, T.-J. Zhu and X.-B. Zhao, *Electrochim. Acta*, 2012, **66**, 271–278.

38 A. Ali, E. Y. Hwang, J. Choo and D. W. Lim, *Analyst*, 2018, **143**, 2604–2615.

39 E. A. Dil, M. Ghaedi and A. Asfaram, *Ultrason. Sonochem.*, 2017, **34**, 792–802.

40 A. Asfaram, M. Ghaedi and M. K. Purkait, *Ultrason. Sonochem.*, 2017, **38**, 463–472.

41 M. Dastkhoon, M. Ghaedi, A. Asfaram, M. Arabi, A. Ostovan and A. Goudarzi, *Ultrason. Sonochem.*, 2017, **36**, 42–49.

42 M. Fu, H. Xing, X. Chen, F. Chen, C. M. Wu, R. Zhao and C. Cheng, *J. Chromatogr. A*, 2014, **1369**, 181–185.

43 X. Yang, P. Zhang, X. Li, L. Hu, H. Gao, S. Zhang, W. Zhou and R. Lu, *Talanta*, 2016, **153**, 353–359.

44 A. Asfaram, M. Ghaedi, H. Javadian and A. Goudarzi, *Ultrason. Sonochem.*, 2018, **47**, 1–9.

45 A. Asfaram, M. Arabi, A. Ostovan, H. Sadeghi and M. Ghaedi, *New J. Chem.*, 2018, **42**, 16144–16153.

46 A. Asfaram, M. Ghaedi and M. Purkait, *Ultrason. Sonochem.*, 2017, **38**, 463–472.

47 H. Wang, G. J. Provan and K. Helliwell, *Food Chem.*, 2004, **87**, 307–311.

48 M. Arabi, A. Ostovan, A. Asfaram and M. Ghaedi, *New J. Chem.*, 2018, **42**, 14340–14348.

49 R. Liu, J. Zhou and A. Wilding, *J. Chromatogr. A*, 2004, **1022**, 179–189.

50 J. L. Zhou, K. Maskaoui and A. Lufadeju, *Anal. Chim. Acta*, 2012, **731**, 32–39.

51 N. Jalilian, H. Ebrahimzadeh and A. A. Asgharinezhad, *Microchem. J.*, 2018, **143**, 337–349.

52 C. Kohlert, G. Abel, E. Schmid and M. Veit, *J. Chromatogr. B: Anal. Technol. Biomed. Life Sci.*, 2002, **767**, 11–18.

53 A. Cantalapiedra, M. Gismera, M. Sevilla and J. R. Procopio, *Phytochem. Anal.*, 2014, **25**, 247–254.